Environmental Science & Technology

pubs.acs.org/est

Article

Rates of Abiotic Mn^{II} Oxidation by O_2: Influence of Various Multidentate Ligands at High pH

James J Morgan, Mark A Schlautman,* and Halka Bilinski

Cite This: *Environ. Sci. Technol.* 2021, 55, 14426−14435

Read Online

ACCESS | Metrics & More | Article Recommendations | Supporting Information

ABSTRACT: Oxidation of manganous manganese (Mn^{II}) is an important process driving manganese cycles in natural aquatic systems and leading to the formation of solid-phase $Mn^{III,IV}$ (hydr)oxide products. Previous research has shown that some simple ligands (e.g., phosphate, sulfate, chloride, fluoride) can bind with Mn^{II} to make it unreactive to oxidation by dissolved oxygen. However, there is little to no understanding of the role played by stronger, complex-forming ligands in Mn^{II} oxidation reactions. The objective of this study was to evaluate the rates of abiotic Mn^{II} oxidation by O_2 in the presence of low concentrations of several complex-forming model ligands (pyrophosphate, tripolyphosphate, ethylenediaminetetraacetic acid, oxalate) in bicarbonate-carbonate buffered laboratory solutions of pH 9.42, 9.65, and 10.19. The influence of increasing ligand concentrations on observed autocatalytic profiles of Mn^{II} oxidation was investigated, and initial oxidation rates were linked quantitatively to the initial Mn^{II} speciation in experimental solutions. Observed rates of Mn^{II} oxidation decreased with increasing ligand concentration for all four ligands tested. However, the profiles observed with time and the magnitudes of decrease in initial oxidation rates were different for the different ligands. Likely explanations for these observations include the denticity of the tested ligands, the relative strength of the ligands to complex Mn^{II} versus Mn^{III}, and the ability of some ligands to enhance the reduction of Mn^{III} back to Mn^{II} on a time scale comparable to the forward homogeneous Mn^{II} oxidation reaction.

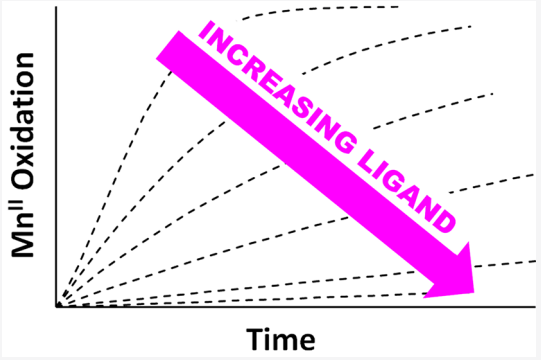

KEYWORDS: *manganese, oxidation, ligand, dissolved oxygen, autocatalysis, redox reaction*

1. INTRODUCTION

Manganese (Mn) has a global abundance of roughly 0.1%, making it the tenth-most abundant element on Earth.[1] It is an essential trace element for plant and animal life, present as a metal cofactor in approximately 6% of all known metal-loenzymes including being the primary electron acceptor in the oxidation of water in photosystem II.[2] Manganese is widely distributed in aqueous systems (e.g., rivers, lakes, reservoirs, groundwaters, estuaries, ocean waters)[1,2] and thus is an element of interest to many complementary fields of aquatic science and engineering. In natural aquatic environments, Mn typically will be found in its II, III, and IV oxidation states.

Manganese cycles in aquatic systems often are driven by reaction of dissolved Mn^{II} and O_2, typically producing solid (hydr)oxide products such as MnOOH, Mn_3O_4, and $MnO_{1.7-1.9}$.[3−8] The oxidation of dissolved Mn^{II} by O_2 is strongly pH dependent and first-order with respect to the metal ion.[6] Although a number of oxidation mechanisms have been proposed to account for the observed rate behavior, the most generally accepted stepwise oxidation scheme is the Haber-Weiss mechanism whereby the overall four-electron reduction of O_2 to H_2O occurs via the reactive intermediate species superoxide radical anion (O_2^-), hydrogen peroxide (H_2O_2), and the hydroxyl radical ($OH^•$).[2,6,9] The first step in the Haber-Weiss sequence, electron transfer from the metal ion to O_2 and formation of O_2^-, is generally rate-limiting and considered to be the elementary reaction that controls the overall rate of metal oxidation.[2,6,9] The precipitated solid products of Mn^{II} oxidation may be involved subsequently in transport of other metal ions to sediments[10] and can play an important role in the oxidation of natural and contaminant organic or inorganic compounds.[11−13]

1.1. Reactive vs Unreactive Mn^{II} Species.

Morgan has reviewed various pathways and time scales of Mn^{II} oxidation by dissolved oxygen and developed a kinetic rate expression for the homogeneous oxidation of Mn^{II} that considered both reactive and unreactive species over the pH range of 8−9.3.[6] Abiotic oxidation reactions yielding $Mn^{III,IV}$(hydr)oxides are often more rapid in higher pH natural waters. The explanation for this observation lies in the pH and alkalinity dependence of Mn^{II} species which are reactive with O_2. For observations in

Special Issue: Tribute to James J. Morgan

Received: March 27, 2021
Revised: June 3, 2021
Accepted: June 22, 2021
Published: July 7, 2021

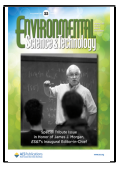

seawater and in laboratory solutions utilizing carbonate and ammonia buffers, Morgan employed a *species reactivity−species fraction model*[14] to fit observed first-order rate constants for oxidative disappearance of total aqueous Mn^{II}.[6] Morgan assumed each reactive species of Mn^{II} present in solution (Mn^{II}_i) had a unique *elementary reaction* rate constant (k_i, units of M^{-1} s^{-1}) for the *rate-determining first step* in the required *four-electron reduction* of O_2:

$$O_2 + Mn_i^{II} \rightarrow O_2^- + Mn_i^{III} \quad (1)$$

where each Mn^{II} species fraction is determined by $\alpha_i = [Mn^{II}_i]/[Mn^{II}]_T$. Morgan then demonstrated that the observed first order rate constant for Mn^{II} disappearance, that is, oxidation to Mn^{III}, in a homogeneous solution "j" is related to the elementary species rate constants and the equilibrium species fractions in solution by the expression: [6]

$$k_j = 4 \sum \alpha_{ij} k_i \quad (2)$$

For low Mn^{II} concentrations over the pH range 8 to 9.3, Morgan deduced that the solution species $MnOH^+$, $Mn(OH)_2^0$, and $Mn(CO_3)_2^{2-}$ are reactive with $O_2(aq)$.[6] Fitting of observed first-order Mn^{II} disappearance rate constants together with known species fractions in eq 2 yielded elementary reaction rate constants for species $MnOH^+$, $Mn(OH)_2^0$ and $Mn(CO_3)_2^{2-}$. For example, in the first of four sequential one-electron reactions between O_2 and $Mn(OH)_2^0$

$$Mn^{II}(OH)_2^0(aq) + O_2(aq) \rightarrow Mn^{III}(OH)_2^+(aq) + O_2^-(aq) \quad (3)$$

the species rate constant was found to be ∼20 M^{-1} s^{-1}.

The reactive species fractions are functions of ionic strength, temperature, pH, dissolved inorganic carbon, alkalinity, etc. Species rate constants depend on temperature. More generally, Mn^{II} species unreactive with O_2 also must be taken into account because the sum of all Mn^{II} species fractions is unity. The presence of ligands forming *unreactive* Mn^{II} complexes diminishes the reactive species fractions, thereby lowering the rate of oxidative Mn^{II} disappearance. Among such ligands, based on previous observations, are phosphate, sulfate, chloride, perchlorate, and fluoride.[1,15] If solution conditions and pertinent equilibrium constants are known, speciation in initial Mn^{II} solutions can be determined using aqueous equilibrium computer programs.[6]

1.2. Mn^{II} Oxidation vis-à-vis Mn^{II} Disappearance/Removal from Solution. Consider the overall reaction

$$4Mn^{II}(aq) + O_2(aq) + 6H_2O \rightarrow 4Mn^{III}OOH(s) + 8H^+ \quad (4)$$

in which four electrons are transferred to O_2, with each of four Mn^{II} atoms surrendering an electron, thereby forming Mn^{III} ions in the solid product. The observed rate expression for Mn^{II} disappearance at lower concentrations of Mn^{II} and lower pH is[16,17]

$$-d[Mn^{II}(aq)]/dt = k_{app}[O_2][Mn^{II}] = k_{1,dis}[Mn^{II}] \quad (5)$$

which is equal to the rate of (hydr)oxide product formation, $d[Mn^{III}OOH(s)]/dt$. MnOOH(s) has been observed as the major solid product of Mn^{II}+O_2 at pH of 9 and below.[4,18] We adopt the convention that total *equivalents* (moles of electron deficiency) of oxidized Mn are counted with respect to the Mn^{II} level as a reference and write

$$[OxMn] = [Mn^{III}] + 2[Mn^{IV}] \quad (6)$$

where [OxMn] is the *equivalent concentration* (eq/L) of oxidized Mn in solid product.

For the stoichiometry of the schematic reaction in eq 4, the rates of Mn^{II} disappearance and oxidation are equal, that is, $-d[Mn^{II}]/dt = d[Mn^{III}OOH]/dt = d[OxMn]/dt$. However, if the oxidation product is $Mn_3O_4(s)$:

$$3Mn^{2+}(aq) + {}^1/_2 O_2(aq) + 3H_2O \rightarrow Mn_3O_4(s) + 6H^+ \quad (7)$$

then the rates of Mn^{II} disappearance and oxidation are *not* equal because each mole of $Mn_3O_4(s)$ contains *two* Mn^{III} ions and *one* Mn^{II} ion. Hence, the rate of *oxidation* of Mn^{II} is $^2/_3$ the rate of Mn^{II}*disappearance* from solution.

Various solid products have been reported to form as a result of Mn^{II} oxidation, including MnOOH (manganite, feitknechtite, groutite), Mn_3O_4 (hausmannite), and MnO_2 (birnessite). At short reaction times, the initial products formed may be amorphous solids and not yet well-defined mineral phases.[7,15] In some cases, the solid products are reported as MnO_x, where x = O/Mn is the experimentally determined stoichiometric coefficient that indicates the average oxidation state (AOS) of Mn in the solids (i.e., Mn-AOS = $2x$). Likewise, x tracks with the equivalent concentration of Mn in the solid product normalized by the total solid-phase Mn concentration (i.e., $[OxMn]/[MnOx] = 2x - 2$). For Mn^{II} oxidation by O_2, the value of x generally ranges from ∼1.3 to ∼2. For example, x = 1.33, 1.5, and 2 (i.e., $MnO_{1.33}$, $MnO_{1.5}$ and MnO_2) would be the expected values for hausmannite, manganite and birnessite, respectively. Progressive oxidation of Mn^{II} (aq) over 175 days with pH changing from ∼9.1 to 8.92 in ammonia buffer revealed that the stoichiometric ratio of O to Mn in the solid product increased from $MnO_{1.37}$ to $MnO_{1.49}$.[5] The product after 7 days comprised 74% Mn^{III} and 26% Mn^{II}.

1.3. Catalysis by (Hydr)Oxide Products. At pH values ranging from ∼9 to 9.3 and total Mn^{II} concentrations above ca. 20 μM, previous observations showed that reaction between $Mn^{II}(aq)$ and $O_2(aq)$ yields as oxidation products Mn^{III} or Mn^{IV} oxides, for example, MnOOH, Mn_3O_4, MnO_2, or, more generally, MnO_x which then may catalyze a surface reaction between Mn^{II} and oxygen.[1,15,19] The overall oxidation process is then autocatalytic, that is, the rate of the reaction is increased by the product.[1,20−22] Effects of ligands on oxidation rates therefore need to be assessed in an autocatalysis context. A framework may be visualized with the following *schematic reaction sequence* with Mn_3O_4 as an example product (reactions not balanced in detail):

$$Mn^{II}(aq) + O_2(aq) \rightarrow Mn_3O_4(s). . \quad (8)$$

$$Mn_3O_4(surface) + Mn^{II}(aq) \Leftrightarrow Mn_3O_4{\cdot}Mn^{II}(surface) \quad (9)$$

$$Mn_3O_4{\cdot}Mn^{II}(surface) + O_2(aq) \Leftrightarrow Mn_3O_4{\cdot}Mn^{II}{\cdot}O_2(surface) \quad (10)$$

$$Mn_3O_4{\cdot}Mn^{II}{\cdot}O_2(surface) \rightarrow Mn_3O_4(s). . \quad (11)$$

Reaction 8 represents homogeneous solution oxidation. Reaction 9 pictures rapid adsorption of aqueous Mn^{II} to the surface of the oxide product, paced by the high water exchange rate of $Mn^{2+}(aq)$.[23] Reaction 10 represents adsorption of

https://doi.org/10.1021/acs.est.1c01795
Environ. Sci. Technol. 2021, 55, 14426−14435

O_2(aq) to an (hydr)oxide surface site holding adsorbed Mn^{II}. Reaction 11 is oxidation of surface Mn^{II}, thereby forming more oxide product. Such a sequence is subject to *potential ligand influences* on rates, viz, (i) slowing or speeding Reaction 8 by complexing Mn^{2+}(aq); (ii) altering the rate of Mn^{II}(aq) adsorption, Reaction 9; (iii) reductive dissolution of the Mn^{III} oxide by a redox-active solution species (e.g., oxalate ion); and (iv) ligand-assisted dissolution of the Mn^{III} oxide by a ligand in solution (e.g., pyrophosphate or citrate).

1.4. Autocatalysis Rate Expressions. The foregoing oxidation reaction scheme (Reactions 8 through 11) is consistent with the phenomenological rate expression proposed to track the apparent autocatalytic oxidative disappearance of Mn^{II} from solution:[1,15]

$$-d[Mn^{II}(aq)]/dt = k_1[Mn^{II}(aq)] + k_2[Mn^{II}(aq)][MnO_x] \quad (12)$$

wherein the coefficients k_1 and k_2 are pseudo order rate constants that are functions of experimental variables such as temperature, pH, Mn^{II}(aq) species, oxygen concentration, ionic strength and properties of the (hydro)oxide MnO_x product (e.g., specific surface).[1,6,23] The model assumes that Mn^{II} adsorbed to the oxide surface is small with respect to the Mn^{II} in solution and the manganese contained in the product MnO_x. Sung and Morgan reported that reaction between Fe^{II} and O_2 also could proceed autocatalytically in accordance with eq 12 and derived an integrated solution for the above differential equation, recast below for the disappearance of Mn^{II} from solution as a function of time:[24]

$$[Mn^{II}(aq)] = \frac{[Mn^{II}]_0(k_1 + k_2[Mn^{II}]_0)}{k_2[Mn^{II}]_0 + k_1\exp\{(k_1 + k_2[Mn^{II}]_0)t\}} \quad (13)$$

where $[Mn^{II}]_0$ is the initial Mn^{II} concentration in solution at the beginning of the oxidation reaction. Morgan used a logarithmic form of eq 13 and an iterative procedure to obtain resolved sets of values for the homogeneous and heterogeneous rate constants, k_1 and k_2, respectively, describing Mn^{II} oxidation by O_2 in bicarbonate and ammonia buffer solutions with pH ranging from 9 to 9.3.[6] Mata-Perez and Perez-Benito demonstrated generic use of the logarithmic form of the integrated solution to fit experimental observations and extract rate constants for other types of autocatalytic reactions.[25]

1.5. Potential Effects of Complexing Ligands on Mn^{II} Oxidation. Effects that ligands may have on Mn^{II} oxidation by O_2 generally can be attributed to (1) Mn^{II}–ligand complexes in solution, (2) Mn^{III}-ligand complexes in solution, and/or (3) ligand adsorption on MnO_x surface sites followed by subsequent reaction(s). For example, Mn^{II} complex species that form with strong ligands will lower the concentrations of O_2-reactive Mn^{II} species such as $MnOH^+$ or $Mn(OH)_2^0$. If these ligand complexes of Mn^{II} are unreactive or more slowly reacting, then the overall observed rate of Mn^{II} oxidation will become slower in the presence of the ligand. If the ligand complexes of Mn^{II} are more rapidly reacting, however, then the overall observed rate of Mn^{II} oxidation will increase when the ligand is present. It has been reported previously that orthophosphate, sulfate, chloride, fluoride, ammonia and humic acids all lead to slower rates of oxidation of Mn^{II} by O_2.[1,6,15,26] Ligands such as tartrate, citrate and desferrioxamine B, however, have been observed to enhance Mn^{II} oxidation by O_2.[27−29]

Once Mn^{II} oxidation has occurred, ligand complexes with Mn^{III} may be present in aqueous solution[30] which will increase the overall solubility of Mn^{III} and decrease formation of oxidized Mn solid products, MnO_x, that otherwise might catalyze further Mn^{II} oxidation. Additional homogeneous reactions are possible for the Mn^{III}–ligand complexes. For example, Kostka et al. reported that Mn^{III}–pyrophosphate complexes were rapidly reduced abiotically by dissolved Fe^{II} or dissolved sulfide in the absence of oxygen.[31] In oxygenated systems, Klewicki and Morgan reported that Mn^{III}–pyrophosphate complexes decomposed very slowly via ligand hydrolysis and disproportionation, whereas citrate and EDTA complexes with Mn^{III} resulted in more rapid decomposition due to electron transfer from the organic ligands to Mn^{III}.[28] Oldham et al. reported that natural Mn^{III}–ligand complexes are abundant in some oxygenated waters and can be expected to participate in a variety of redox reactions and biogeochemical processes.[32]

When oxidized Mn solid products do form, ligands present in solution may adsorb to sites on MnO_x surfaces which can lead to subsequent reactions such as ligand-promoted dissolution of MnO_x solids[33,34] and/or reductive dissolution of MnO_x solids.[33−36] Ligand-promoted dissolution was reported for β-MnOOH with pyrophosphate[33] and for Mn_3O_4 by desferrioxamine B above pH 8.[34] Examples of the reductive dissolution of MnO_x solids include MnO_2 by the microbial metabolites oxalate and pyruvate,[35] γ-MnOOH with several aminocarboxylate ligands including EDTA,[36] β-MnOOH with the ligands EDTA and citrate,[33] and Mn_3O_4 by desferrioxamine B below pH 8.[34]

1.6. Research Objectives and Rationale. In this paper, we report original experimental results of the kinetics of abiotic Mn^{II} oxidation by dissolved oxygen in the presence of low concentrations of several model complex forming ligands in bicarbonate–carbonate buffered laboratory solutions. The objectives of our study were to qualitatively investigate the influence of increasing ligand concentrations on observed autocatalytic profiles of Mn^{II} oxidation, and to quantitatively link initial oxidation kinetics to the Mn^{II} speciation at the start of the reactions. Our aim was to achieve appreciable levels of Mn^{II} oxidation over reaction times of approximately 1–2 h, which could be achieved by maintaining a constant partial pressure of 1 atm O_2 throughout the oxidation reaction and by utilizing appropriate experimental conditions for pH (9.4–10.2) matched with initial total Mn^{II} (200–50 μM) to take advantage of the faster rate of Mn^{II} oxidation with increasing pH. Four model ligands were chosen: pyrophosphate and tripolyphosphate, as examples of nonredox active inorganic ligands; and EDTA and oxalate, as examples of potentially redox active organic ligands. Condensed phosphates (e.g., pyrophosphate, tripolyphosphate) and EDTA are ligands often associated with water contamination, whereas oxalate is a naturally occurring ligand found in aquatic systems as a consequence of biological activity. The denticity of the four selected ligands also varies, from bidentate (pyrophosphate and oxalate) to tridentate (tripolyphosphate) to hexadentate (EDTA).

2. MATERIALS AND METHODS

2.1. Reagents. Twice-distilled water was used to prepare all solutions. Chemicals purchased were reagent grade or better and used as received: manganese perchlorate ($Mn(ClO_4)_2 \cdot 6H_2O$, GFS Chemical); sodium pyrophosphate ($Na_4P_2O_7 \cdot$

https://doi.org/10.1021/acs.est.1c01795
Environ. Sci. Technol. 2021, 55, 14426−14435

$10H_2O$, J.T. Baker); sodium hydroxide (NaOH, Reagent A.C.S. Code 2255, General Chem. Div.); perchloric acid ($HClO_4$, GFS Chemical); sodium tripolyphosphate ($Na_5P_3O_{10}$, Alfa Inorganics Inc.); sodium ethylenediaminetetraacetate (EDTA, $Na_2C_{10}H_{14}N_2N_2O_8{\cdot}2H_2O$, J.T. Baker); sodium oxalate ($Na_2C_2O_4$, J.T. Baker); sodium carbonate (Na_2CO_3, Aldrich); sodium bicarbonate ($NaHCO_3$, Aldrich); glacial acetic acid (AnalR); and leuco crystal violet (Sigma-Aldrich). USP-grade oxygen gas was used to presaturate all reaction solutions, and a constant partial pressure of 1 atm O_2 was maintained by continuous bubbling of the solutions with oxygen gas throughout the experiments.

2.2. Mn^{II} Oxidation Experiments. Mn^{II} oxidation experiments at P_{O2} = 1 atm were conducted in a 1000 mL standard Pyrex beaker at room temperature (22 °C) and ambient laboratory light; dark controls were not utilized because normal laboratory light had no observed effect on Mn^{III}–EDTA reactions.[28] Solutions were mixed using a Teflon coated magnetic stirring bar at 60 rpm. Pure O_2 was bubbled for 30 min prior to initiating the oxidation reaction, and continuous bubbling was maintained throughout the experiments. Reaction solutions were created with specified concentrations of Na_2CO_3 and $NaHCO_3$ chosen to yield pH values of 9.42, 9.65, or 10.19. Total carbonate component concentrations were 0.010 M, and a Radiometer 25 (Copenhagen, Denmark) pH meter with glass/reference electrode pair, calibrated on the NBS buffer scale, was used to measure pH. The ionic strength was 0.014 M at pH 9.42, 0.015 M at pH 9.65, and 0.020 M at pH 10.19. Sodium salts of the individual ligands pyrophosphate, EDTA, oxalate, or tripolyphosphate were added to give a known initial concentration of each ligand. A pipet (TD) was used to rapidly add 10.0 mL of an appropriate $Mn(ClO_4)_2$ working solution. Working solutions of 1.0, 2.0, 5.0, 6.25, or 10.0 mM were employed for adding 10.0 mL of Mn^{II} solution immediately above the liquid surface, near the center of the stirred reactor.

The course of the oxidation reaction was followed by withdrawing 10.0 mL samples at regular intervals extending from about 5 to 120 min. Samples withdrawn were quenched immediately in a 100 mL flask containing pH 4.0 acetate buffer with leuco crystal violet (LCV) reagent.[37] Visible spectrophotometry (Beckman Model DU Quartz Spectrophotometer with quartz cells of path length 10, 5, 2, and 1 cm) was used to determine the concentration of oxidized manganese after dilution to the mark. The molar absorptivity of oxidized crystal violet, $(7.9 \pm 0.2) \times 10^4$ $M^{-1}cm^{-1}$, was determined with a series of dilute synthetic colloidal suspensions of MnO_2 that had been standardized by iodometry. The LCV method was used to measure the reaction advancement, i.e., oxidized manganese equivalent concentration (denoted by [OxMn] = $[Mn^{III}] + 2[Mn^{IV}]$ in eq/L) vs time. Manganese in oxidation states III and IV, either as particles (e.g., Mn_3O_4, MnOOH, MnO_2) or aqueous species (e.g., $Mn^{III}P_2O_7$), can oxidize the leuco form of crystal violet (LCV) to its intensely colored dye form (CV) in pH 4.0 acetate buffer with loss of two electrons. The formation of CV is rapid.[37] For example, Johnson and Chiswell observed that oxidation of a 50 μM LCV reagent solution at pH 4.0 to CV by a 4.5 μM colloidal suspension of colloidal MnO_2 particles required less than 2 min.[38]

2.3. Data Analysis. When the progress of $Mn^{II}(aq)$ oxidation by O_2 is tracked by measurements of the equivalent oxidation concentration of product, [OxMn], an integrated solution analogous to eq 13 can be derived:

$$[\mathrm{OxMn}] = [\mathrm{OxMn}]_{max} - \frac{[\mathrm{OxMn}]_{max}(k_1 + k_2[\mathrm{OxMn}]_{max})}{k_2[\mathrm{OxMn}]_{max} + k_1\exp\{(k_1 + k_2[\mathrm{OxMn}]_{max})t\}} \quad (14)$$

where $[\mathrm{OxMn}]_{max}$ is the maximum possible equivalent concentration of electron deficiency in the specific oxidized Mn products formed. In other words, $[\mathrm{OxMn}]_{max}$ depends not only on the initial Mn^{II} concentration but also on the particular MnO_x product stoichiometry. In results presented here for Mn^{II} oxidation experiments, with reaction times of ca. 2 h at 22 °C, the products expected are $MnO_{1.33\pm0.05}$ at pH 9.42 and 9.65, and $MnO_{1.75\pm0.05}$ at pH 10.19.[1,3,15,27] eq 14 was fitted to the experimentally determined concentrations of [OxMn] vs time using nonlinear least-squares regression (JMP Pro 14.3.0, SAS Institute Inc., 2018). Fitting of each experimental data set over the entire reaction period enabled values to be obtained for k_1, k_2, and $[\mathrm{OxMn}]_{max}$, although the value of $[\mathrm{OxMn}]_{max}$ was more commonly fixed during fitting to be consistent with the MnO_x product stoichiometries reported above because plateaus in [OxMn] were obtained in only a limited number of experiments. For the results described herein, the fitting procedure we used emphasized earlier time points together with fixed $[\mathrm{OxMn}]_{max}$ values so that we could obtain the most reliable estimates of k_1 possible, which we then could compare against the known chemical speciation that existed for the initial experimental conditions. It is important to note that although estimates of k_2 changed slightly depending on the particular value selected for $[\mathrm{OxMn}]_{max}$, the fitted estimates of k_1 were independent of the fixed $[\mathrm{OxMn}]_{max}$ value selected. Goodness of fit was evaluated based on residual plots, sum of squared errors (SSE), root mean squared errors (RMSE), and uncertainties in the fitted parameter values.

2.4. Mn^{II} Speciation in Initial Solutions. The equilibrium constants used to calculate initial concentrations and Mn^{II} species fractions in the various experimental systems are reported in Table 1. These infinite dilution stability constants were used together with the Davies equation[2] to make activity corrections and species calculations appropriate for the ionic strengths and other solution conditions of the experiments.

3. RESULTS AND DISCUSSION

3.1. Autocatalytic Profiles of Mn^{II} Oxidation by O_2. Time profiles for the oxidation of Mn^{II} by oxygen, as tracked by the concentration of [OxMn] produced, are shown in Supporting Information (SI) Figures S1–S3 for the different experimental conditions tested. Using pyrophosphate at pH 10.19 as an example (Figure 1), the rate of Mn^{II} oxidation slows down appreciably with increasing ligand concentration: the oxidation profile curves shift to the right and down with increasing dose of pyrophosphate from zero up to the initial stoichiometric ratio $[L]_T/[Mn^{II}]_T$ = 1. In the absence of pyrophosphate, oxidation of 50 μM Mn^{II} plateaus at $[\mathrm{OxMn}]_{max}$ = 72.2 μeq/L after ca. 40 min (Figure 1). If all of the initial Mn^{II} has been oxidized at this point, then the solid product would have Mn-AOS = 3.44 and a stoichiometric formula equivalent to $MnO_{1.72}$. Figure 1 shows that 50% of $[\mathrm{OxMn}]_{max}$ is reached in approximately 16, 27, and 50 min for pyrophosphate concentrations of 0, 10, and 15 μM, respectively. For 25 μM pyrophosphate, extrapolation of the curve indicates that more than 2 h would be needed to reach 50% of $[\mathrm{OxMn}]_{max}$. For 40 and 50 μM pyrophosphate, it is

https://doi.org/10.1021/acs.est.1c01795
Environ. Sci. Technol. 2021, 55, 14426−14435

Table 1. Equilibrium Reaction Constants (Infinite Dilution, 25°C) Used to Determine Initial Species Concentrations in the Various Mn^{II} Experimental Systems

reaction	log K_{eq} [a]
$H_2O = H^+ + OH^-$	−14.00
$CO_2(aq) + H_2O = HCO_3^- + H^+$	−6.35
$HCO_3^- = CO_3^{2-} + H^+$	−10.33
$Mn^{2+} + H_2O = MnOH^+ + H^+$	−10.60
$Mn^{2+} + 2H_2O = Mn(OH)_2 + 2H^+$	−22.20
$Mn^{2+} + 3H_2O = Mn(OH)_3^- + 3H^+$	−34.80
$Mn^{2+} + 4H_2O = Mn(OH)_4^{2-} + 4H^+$	−48.30
$Mn^{2+} + CO_3^{2-} = MnCO_3(aq)$	4.40
$Mn^{2+} + 2CO_3^{2-} = Mn(CO_3)_2^{2-}$	5.70
$Mn^{2+} + CO_3^{2-} + H^+ = MnHCO_3^+$	11.60
$Mn^{2+} + CO_3^{2-} + H_2O = MnOHCO_3^- + H^+$	−6.10

log K_{eq} for Mn^{2+} and strong complexing ligands, L^{n-}

L^{n-}=	$P_2O_7^{4-}$	$EDTA^{4-}$	$P_3O_{10}^{5-}$	Ox^{2-}
L + H = LH	9.40	10.948	9.25	4.266
LH + H = LH_2	6.70	6.273	6.54	1.25
LH_2 + H = LH_3	2.28	3.117	2.37	
L + Mn^{2+} = MnL	6.51[c]	15.61	9.90	3.95

[a]Infinite dilution constants reported by Morgan.[6] [b]Unless otherwise indicated, the infinite dilution constants for the strong complexing ligands have been critically selected from references.[2,39−41] For simplicity, reactions are shown without charge balance. [c]Infinite dilution constant from Bilinski.[42]

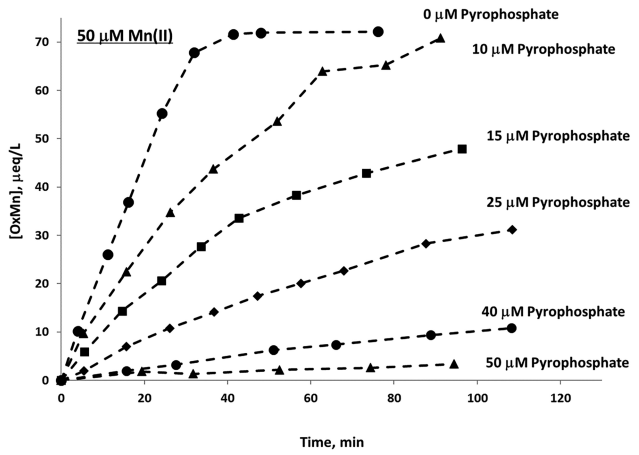

Figure 1. Time profiles of Mn^{II} oxidation by O_2 at pH 10.19 in the absence and presence of pyrophosphate. All solutions had an initial concentration of 50 μM $Mn^{II}(aq)$ and initial pyrophosphate concentrations are shown by their respective curves.

unclear whether the two curves would ever reach 50% of $[OxMn]_{max}$. Qualitative comparison of SI Figures S1−S3 reveals that all of the ligands tested slow down Mn^{II} oxidation under all three pH conditions, albeit to varying extents. For example, as the initial stoichiometric ratio of $[L]_T/[Mn^{II}]_T$ approaches 1 at pH 10.19, EDTA, tripolyphosphate and pyrophosphate nearly completely shut down Mn^{II} oxidation by O_2, whereas 50 μM oxalate only slows down the oxidation rate by about half (SI Figure S1).

Previously, Morgan reported that pyrophosphate ligand in 50-fold excess blocked oxidation of Mn^{II} by O_2 over a period of at least 3 h.[15] In the presence of oxalate or humic acid at pH 9 in borate buffers, oxidation of Mn^{II} to MnO_x solids was slowed appreciably.[26] In considering the effects of ligands, whether "weak" or "strong," on the $Mn^{II}(aq)$ + O_2 reaction, it is important first to recognize that electron transfer from Mn^{II} to O_2 *must* occur through an inner-sphere bond because an outer-sphere process is symmetry-forbidden.[6,9,23] Thus, a ligand which denies access of O_2 to the Mn^{II} metal center, for example, a hexadentate ligand such as EDTA, will prevent electron transfer. Second, ligands able to donate electrons to the Mn^{II} metal center, thereby increasing its reducing power, for example, $2OH^-$, will assist electron transfer to O_2.

3.2. Influence of Multidentate Ligands on Initial Mn^{II} Oxidation Rates. The four multidentate ligands (EDTA, pyrophosphate, tripolyphosphate, or oxalate) evaluated were added at concentrations equal to or less than the initial Mn^{II} concentration, which ranged from 50 to 200 μM. As described in Section 1.1, one possible effect that might result when a Mn^{II}-complex species is formed with one of these ligands would be to lower the concentrations of O_2-reactive Mn^{II} species, for example, $MnOH^+$ or $Mn(OH)_2(aq)$, thereby slowing the initial oxidation rate if the Mn^{II}−ligand complex itself is unreactive or more slowly reactive with O_2.[6] As explained in Sections 2.3 and 2.4, the chemical species present in solution were known only at the beginning of each experiment. Therefore, while data fitting we focused our efforts primarily on obtaining reliable values of the homogeneous rate constant, k_1, for each experiment. Conceptually, this would be equivalent to taking eq 12 as $t \rightarrow 0$ when the oxidation of Mn^{II} is just beginning:

$$-d[Mn^{II}(aq)]/dt|_{t\rightarrow 0} = d[OxMn]/dt|_{t\rightarrow 0} = k_1[Mn^{II}(aq)]_0 \quad (15)$$

To evaluate the effects of different ligands, different ligand concentrations, different initial Mn^{II} concentrations, and different pH conditions on the initial rate of Mn^{II} oxidation for the various experimental conditions used, it is convenient to normalize all k_1 values by their corresponding homogeneous rate constant when no strong ligand is present (e.g., $k_L/k_{L=0}$). Moreover, it is convenient to normalize the added ligand concentrations by the initial concentration of Mn^{II}, (e.g., the normalized *dose* of ligand-to-Mn^{II}, $[L]_T/[Mn^{II}]_T$]), or by accounting for the fraction of initial Mn^{II} that is complexed by a specific ligand at its added concentration (e.g., $\alpha_{Mn(II)L}$).

Figures 2 and 3 reveal the effects of different normalized ligand doses, and of the initial fraction of ligand-complexed Mn^{II}, respectively, on the normalized homogeneous rate constant, k_1. For all panels shown in these two figures, a negative 1:1 line has been included for comparison with the actual data points from the experiments. The usefulness of graphs like those in Figure 2 are to help determine how the presence of a ligand may affect the initial rate of Mn^{II} oxidation when only total ligand and total Mn^{II} concentrations are measured. In contrast, graphs like those in Figure 3 link changes in the initial rate of Mn^{II} oxidation to the specific fraction of Mn^{II} complexed by the strong ligand.

3.2.1. EDTA. The hexadentate ligand EDTA forms a stable complex with Mn^{2+}, occupying all of the Mn^{II} coordination positions. Of the four ligands studied, EDTA has by far the largest stability constant (Table 1). As such, when EDTA is initially present at or below stoichiometric concentrations, it outcompetes weaker ligands present in solution for that particular fraction of the metal and is itself completely complexed with Mn^{II}. Comparing the upper left panels of Figures 2 and 3, particularly the *x*-axis values of the data points shown, demonstrates the complete complexation of EDTA by

https://doi.org/10.1021/acs.est.1c01795
Environ. Sci. Technol. 2021, 55, 14426−14435

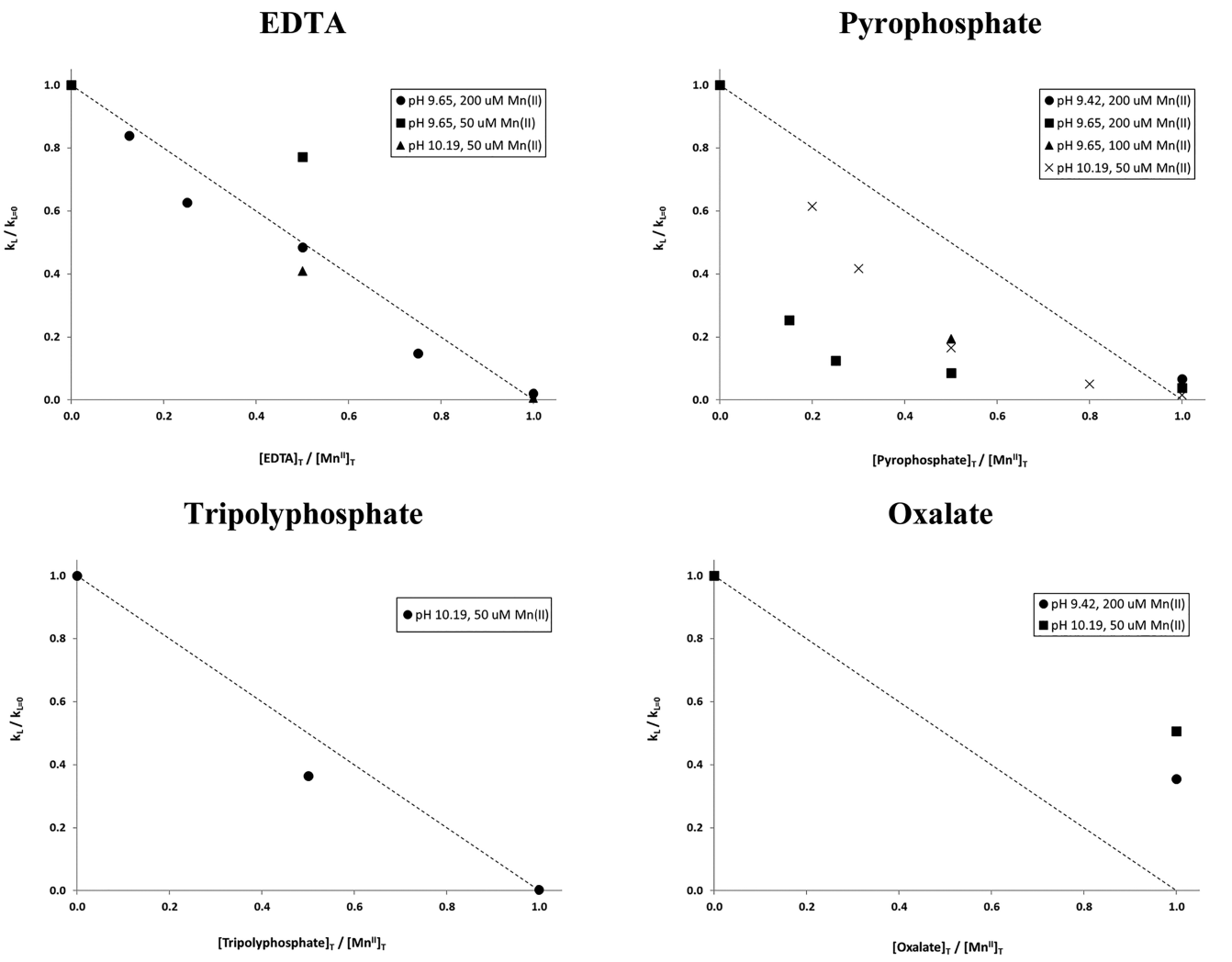

Figure 2. Effects of different strong ligand doses on the normalized homogeneous rate constant, $k_L/k_{L=0}$. Each *x*-axis shows the ratio of added ligand divided by the initial Mn^{II}(aq) concentration, $[L]_T/[Mn^{II}]_T$. Each *y*-axis shows the best fit values of k_1 for each experiment divided by the corresponding experimental condition with no ligand present (see text). The dashed line has a slope of −1.

Mn^{II} at all three pH values in our experiments. Additionally, the *y*-axis values for the data points in these same two upper left panels reveal that the *normalized* homogeneous oxidation rate constants decrease systematically with increasing additions of EDTA and fall very close to the negative 1:1 line, all approaching zero as the EDTA-to-Mn^{II} dose approaches 1 (Figure 2) and the fraction of Mn^{II} complexed by EDTA approaches 1 (Figure 3). Taken together, the results with EDTA demonstrate an *ideal unreactive* ligand effect, namely, the strong hexadentate EDTA ligand effectively converting Mn^{II} species that are reactive with O_2 to a Mn^{II}−EDTA complex species that is unreactive as described in Section 1.1.

It is important to note that the results shown in Figures 2 and 3 pertain to the early stages of the oxidation reaction between Mn^{II} and O_2. As Mn^{II} oxidation proceeds to form Mn^{III} in solution and then subsequently MnO_x solid products at longer reaction times, EDTA will undergo new competitive ligand exchange reactions. For example, it may be possible that Mn^{III}−EDTA complexes in solution will lead to electron transfer from the ligand to Mn^{III}.[28] After MnO_x solids have formed, some fraction of the EDTA may adsorb at surface sites, which can lead to the reductive dissolution of the solids.[33,36] However, the time frames associated with these additional EDTA reactions are expected to be much longer than the early stages of the Mn^{II} oxidation by O_2 reaction, pertinent to what is shown in Figures 2 and 3. For example, extrapolating results from Klewicki and Morgan[28] suggests a half-life of ∼3 days or longer for electron transfer from EDTA to Mn^{III} under the experimental conditions utilized in the present study (i.e., no *excess* EDTA, pH ∼ 9.5).

3.2.2. Pyrophosphate. Results obtained with the bidentate ligand pyrophosphate (upper right panels of Figures 2 and 3) are in marked contrast with EDTA. Although increasing amounts of pyrophosphate do lead to systematic decreases approaching zero for the normalized homogeneous oxidation rate constants, the data points exhibit curvilinear trends and the points themselves fall well below the negative 1:1 line representing the *ideal unreactive* ligand effect in both graphs. In other words, pyrophosphate is *more effective* than EDTA at inhibiting Mn^{II} oxidation by O_2, despite being a weaker ligand with lower denticity. Because pyrophosphate is a weaker ligand (Table 1), differences are observed between its *dose graph* (Figure 2) and its corresponding Mn^{II}*fraction complexed* graph (Figure 3). It is also possible to discern small differences

https://doi.org/10.1021/acs.est.1c01795
Environ. Sci. Technol. 2021, 55, 14426−14435

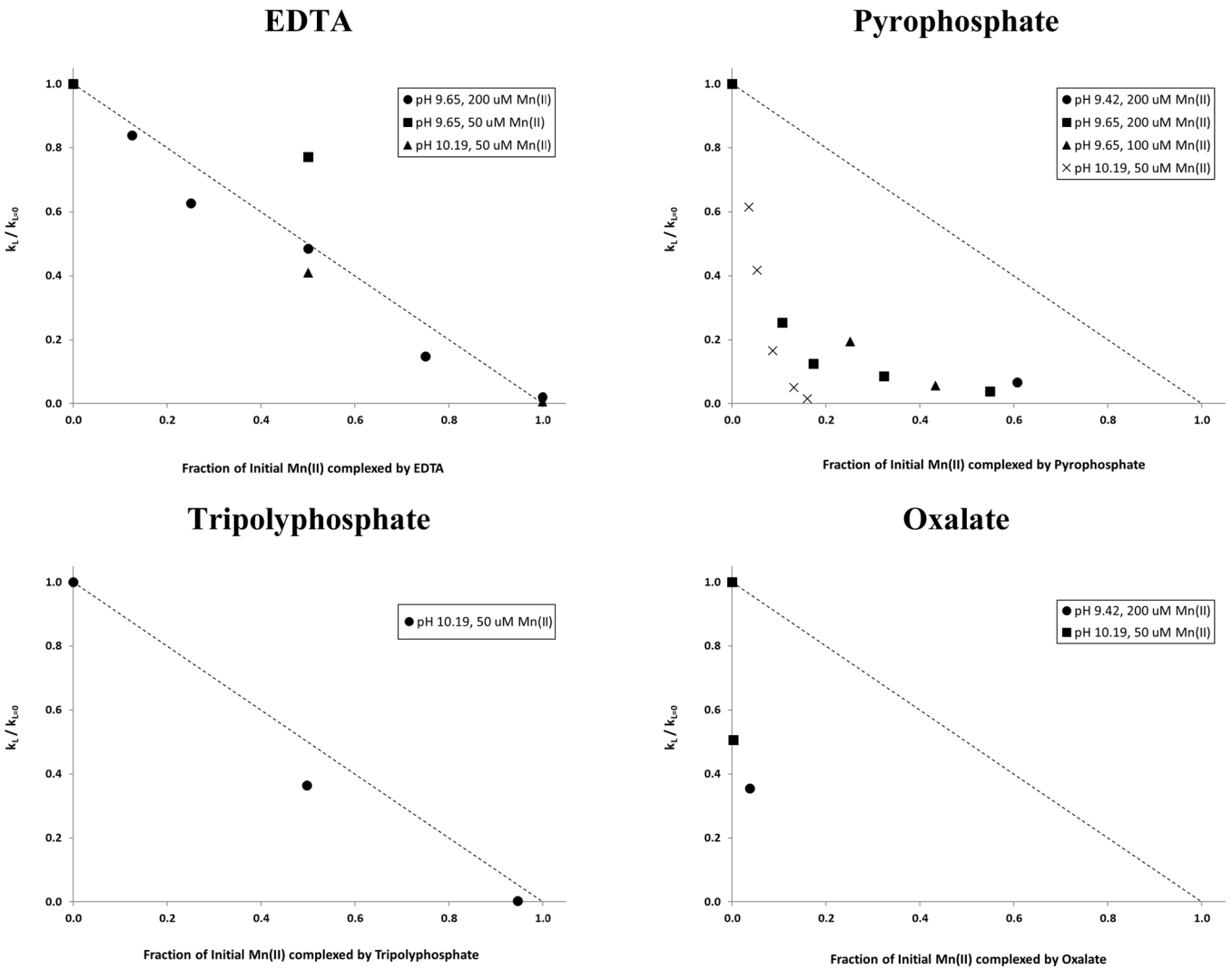

Figure 3. Effects of Mn^{II} complexation by different strong ligands on the normalized homogeneous rate constant, $k_L/k_{L=0}$. Each *x*-axis shows the fraction of initial $Mn^{II}(aq)$ complexed by the specified ligand based on speciation calculations using the equilibrium constants listed in Table 1. Each *y*-axis shows the best fit values of k_1 for each experiment divided by the corresponding experimental condition with no ligand present (see text). The dashed line has a slope of −1, and shows the expected trend if initial complexation by a ligand only converts reactive Mn^{II} to unreactive Mn^{II}.

among the trends obtained with the different pH conditions. For example, when the fraction of Mn^{II} initially complexed by pyrophosphate is ∼60% and less, the ability of pyrophosphate to slow down the overall oxidation reaction increases in the order pH 9.42 < pH 9.65 < pH 10.19 (Figure 3).

It is not obvious how pyrophosphate, considered to be a nonredox active ligand, is able to inhibit the early stages of the Mn^{II} oxidation reaction as effectively as it does. Clearly, there are factors beyond simply converting reactive Mn^{II} species to a Mn^{II}−pyrophosphate complex that is unreactive with O_2 as was observed with EDTA. The possibility that a single pyrophosphate ligand could complex two Mn^{II} atoms was considered but ultimately ruled out as a plausible explanation. Rather, if we accept the stepwise Haber-Weiss mechanism as the scheme describing the overall oxidation of Mn^{II} by O_2,[2,6,9] then other species present in solution (e.g., Mn^{III}−pyrophosphate, O_2^-, H_2O_2) need to be considered. For example, Kostka et al. reported that the Mn^{III}−pyrophosphate complex was an effective environmental oxidant and a stronger oxidant than Mn^{III} complexed to other ligands (e.g., citrate, malate, pyruvate, tiron).[31] Soluble Mn^{III}−pyrophosphate was found to be a potent oxidant for uraninite ($U^{IV}O_2$) at pH 7.5 under low O_2 conditions in the presence of excess pyrophosphate; when the pyrophosphate-to-Mn^{III} ratio decreased from 40 to 6 the reactivity of Mn^{III} increased dramatically with the rate constant tripling.[43] At pH 9, disproportionation of Mn^{III} was observed and the rate of UO_2 dissolution was slightly lower than at pH 7.5.[43]

The superoxide radical anion (O_2^-) is both a one-electron oxidant and a one-electron reductant; it is also unstable and disproportions into O_2 and H_2O_2.[2] In natural waters, O_2^- has been proposed to be an important participant in the redox reactions and cycling of transition metal ions.[2,32,44] Hansard et al.[44] quantified the effect of Mn^{II} on the decay kinetics of O_2^- in authentic seawater samples and in simulated freshwater solutions to which a fulvic acid was added. They also considered the possibility that Mn^{III} could be reduced by O_2^- to reform Mn^{II} and O_2, because that redox reaction is commonly observed with Fe^{II}/Fe^{III}[2] and has been shown to be feasible for Mn^{II}/Mn^{III} from a thermodynamic perspective.[45]

https://doi.org/10.1021/acs.est.1c01795
Environ. Sci. Technol. 2021, 55, 14426−14435

Upon analyzing their data, however, Hansard et al. concluded that Mn^{III} reduction by O_2^- occurred only in a limited number of their seawater experiments when concentrations of O_2^- were higher than the added amount of Mn^{II}.[44] When levels of added Mn^{II} were higher than O_2^-, oxidation to Mn^{III} resulted with no apparent reduction back to Mn^{II}.[44] In a pulse radiolysis study over the pH range 0.1−7.2, reaction of Mn^{II} with O_2^- formed Mn^{III} and H_2O_2 in the presence of excess pyrophosphate to ensure all Mn^{II} existed as a pyrophosphate complex.[46] Therefore, in our experiments it is unlikely that O_2^- would have been able to reduce Mn^{III} back to Mn^{II} in the presence of pyrophosphate.

The possibility that H_2O_2 was acting as a reductant of Mn^{III}−pyrophosphate in our experimental systems may be more plausible.[46] For example, Learman et al. reacted Mn^{II} and O_2^- but observed no measurable amounts of Mn^{III} and Mn^{VI} after several days of reaction.[47] They concluded that absence of $Mn^{III,IV}$ oxide formation was due to reduction of Mn^{III} by H_2O_2, both of which are produced from the reaction between Mn^{II} and O_2^-. When active catalase was added to rapidly decompose H_2O_2 to H_2O and O_2, formation of $Mn^{III,IV}$ oxides was then observed.[47] Addition of excess ligands (pyrophosphate or citrate) to complex Mn^{III} decreased its reduction by H_2O_2 but did not completely eliminate the reductive back reaction; only when catalase was added simultaneously with the excess ligands was the expected increase in Mn^{III} and Mn^{VI} observed.[47] Andeer et al. stated that a requirement for superoxide-mediated $Mn^{III,IV}$ oxide production is the removal of H_2O_2, which inhibits solids formation by reducing Mn^{III}.[48] In a study of Mn^{II} oxidation in Lake Erie, Godwin et al. reported that H_2O_2 acted as a net reductant for manganese oxides and completely masked oxidation of Mn^{II} by O_2^-.[49]

We speculate that the low concentrations of pyrophosphate used in our experiments somehow enhanced reduction of Mn^{III} by H_2O_2. Based on the findings of Klewicki and Morgan,[28,33] we conclude that other possible pyrophosphate-assisted reactions which might have depleted oxidation products (e.g., Mn^{III} or MnO_x) under our experimental conditions would have required much longer reaction times than those pertinent to Figures 2 and 3.

3.2.3. Tripolyphosphate. Fewer experimental data points are available for the nonredox active, tridentate ligand tripolyphosphate (lower left panels of Figures 2 and 3). As a complexing ligand, tripolyphosphate is intermediate between EDTA and polyphosphate with regard to strength of forming a complex with Mn^{II} (Table 1). Based on the limited data, it appears that tripolyphosphate behaves similarly overall to EDTA at slowing down the oxidation reaction between Mn^{II} and O_2. Like EDTA, addition of tripolyphosphate results in a near-linear decrease in the normalized homogeneous rate constant that tracks closely to the negative 1:1 line.

3.2.4. Oxalate. There also are not many data for the bidentate ligand oxalate (lower right panels of Figures 2 and 3), which is the weakest complexing ligand tested in this study (Table 1). When the oxalate dose is equal to the initial Mn^{II} concentration, the normalized homogeneous oxidation rate constant decreases more at pH 9.42 than it does at pH 10.19 (Figure 2). Graphing the normalized rate constant against the initial fraction of Mn^{II} complexed by oxalate (Figure 3), however, provides a better indication of how oxalate may be slowing down the oxidation reaction. Rather than simply converting reactive Mn^{II} to unreactive Mn^{II} as a ligand complex, it appears that the *excess* oxalate initially present in solution (i.e., 96.3% and 99.8% of the total added oxalate is *not* complexed by Mn^{II} at pH 9.42 and 10.19, respectively) may be able to interact with the Mn^{III} formed, both as a complexing ligand and as a reducing agent. If that interpretation is correct, then reduction of Mn^{III} by *excess* oxalate may be occurring similarly to the electron transfer reactions previously reported for Mn^{III} in the presence of *excess* EDTA.[28] Once MnO_x solid products are formed, it may be expected that some of the excess oxalate in solution will be adsorbed by their surfaces, subsequently resulting in reductive dissolution of the solids.[13,35] However, because of the much higher pH conditions used in the present study relative to lower pH ranges examined previously,[13,35] we conclude that oxalate adsorption would be very low in our experiments and that any reductive dissolution of MnOx that might occur would also be very low and negligible for the time frame pertinent to our results in Figures 2 and 3.

3.3. Environmental Implications and Additional Research Needs. As explained in Section 1.6, appreciable levels of Mn^{II} oxidation were achieved within 2 h by using relatively high pH and Mn^{II} concentrations at 1 atm O_2. Although it is possible to encounter similar conditions in some natural aquatic systems or engineered treatment systems (e.g., $[Mn^{II}] > 300\ \mu M$ in selected groundwaters and lakes;[1,50] high pH and O_2 associated with harmful algal blooms[51] or during preaeration and lime treatment for dissolved Mn removal[52]), they would not be considered *typical* aquatic environments.[1,2,32] However, by utilizing a *species reactivity−species fraction* framework[6,14] as described in Section 1.1, our results can be applied to other aquatic environments. The major limitation with extending our results would be how well our model ligands compare to natural ligands in freshwaters, estuaries and the open ocean or to ligands associated with water contamination. Our model ligands ranged in their ability to complex Mn^{II} (Table 1); for comparison, Oldham et al. (and references therein) have classified weak vs strong ligands for Mn^{III} based on log K_{cond} = 13.2.[32] Nevertheless, it is clear that a much better understanding is needed of the nature and abundance of ligands in aquatic environments, particularly their ability to complex and stabilize the various oxidation states of Mn (II, III, and perhaps even IV) and their ability to influence Mn redox thermodynamics and kinetics.[2,28−32] Lastly, we still lack basic information on the amounts of environmental oxidants/reductants (e.g., O_2^-, H_2O_2, $OH^•$, MnO_x) in aquatic systems and their relative importance for Mn cycling, particularly at critical redox boundaries (e.g., the oxic-suboxic interface) and across relevant redox gradients.[2,31,32,44,47−49]

■ ASSOCIATED CONTENT

Supporting Information

The Supporting Information is available free of charge at https://pubs.acs.org/doi/10.1021/acs.est.1c01795.

Text and graphs of time profiles for Mn^{II} oxidation by O_2. *In Jim's own words*: additional text, written ca. 2013, that describes JJM's "odyssey with Mn^{II}, O_2, and ligands" with a closing note by MAS (PDF)

■ AUTHOR INFORMATION

Corresponding Author

Mark A Schlautman − *Department of Environmental Engineering and Earth Sciences, Clemson University,*

https://doi.org/10.1021/acs.est.1c01795
Environ. Sci. Technol. 2021, 55, 14426−14435

Anderson, South Carolina 29625, United States;
orcid.org/0000-0001-6522-4345; Phone: 864-656-4059;
Email: mschlau@clemson.edu; Fax: 864-656-0672

Authors

♦**James J Morgan** − *Department of Environmental Science and Engineering, California Institute of Technology, Pasadena, California 91125, United States*

Halka Bilinski − *Ruđer Bošković Institute, Division for Marine and Environmental Research, HR-10002 Zagreb, Croatia*

Complete contact information is available at:
https://pubs.acs.org/10.1021/acs.est.1c01795

Notes

The authors declare no competing financial interest.
♦Passed away during manuscript preparation.

■ ACKNOWLEDGMENTS

We gratefully acknowledge the constructive comments and suggestions provided by the three anonymous reviewers. Caltech support for emeritus faculty (JJM) helped to make completion of this paper possible. Special thanks go to Alan Stone for his many helpful discussions, and to the many other colleagues, too numerous to mention, who have provided support and guidance. Elements of this paper were presented at the 2020 ACS Fall National Meeting in the Geochemistry Division symposium entitled *Biotic/abiotic Redox Processes of Manganese in Natural and Engineering Systems*, August 16−20.

■ REFERENCES

(1) Morgan, J. J. *Chemistry of Aqueous Manganese II and IV*. Ph.D. thesis, Harvard University, Cambridge, MA, 1964.
(2) Stumm, W.; Morgan, J. J. *Aquatic Chemistry: Chemical Equilibria and Rates in Natural Waters*, 3rd Ed.; Wiley-Interscience: New York, 1996.
(3) Bricker, O. P. Some stability relations in the system Mn-O_2-H_2O at 25°C and one atmosphere total pressure. *Am. Mineral.* **1965**, *50*, 1296−1354.
(4) Hem, J. D. Rates of manganese oxidation in aqueous systems. *Geochim. Cosmochim. Acta* **1981**, *45* (8), 1369−1374.
(5) Murray, J. W.; Dillard, J. G.; Giovanoli, R.; Moers, H.; Stumm, W. Oxidation of Mn(II): Initial mineralogy, oxidation state and ageing. *Geochim. Cosmochim. Acta* **1985**, *49*, 463−470.
(6) Morgan, J. J. Kinetics of reaction between O_2 and Mn(II) species in aqueous solutions. *Geochim. Cosmochim. Acta* **2005**, *69* (1), 35−48.
(7) Toyoda, K.; Tebo, B. M. Kinetics of Mn(II) oxidation by spores of the marine *Bacillus* sp. SG-1. *Geochim. Cosmochim. Acta* **2016**, *189*, 58−69.
(8) Lan, S.; Wang, X.; Xiang, Q.; Yin, H.; Tan, W.; Qiu, G.; Liu, F.; Zhang, J.; Feng, X. Mechanisms of Mn(II) catalytic oxidation on ferrihydrite surfaces and the formation of manganese (oxyhydr)-oxides. *Geochim. Cosmochim. Acta* **2017**, *211*, 79−96.
(9) Rosso, K. M.; Morgan, J. J. Outer-sphere electron transfer kinetics of metal ion oxidation by molecular oxygen. *Geochim. Cosmochim. Acta* **2002**, *66* (24), 4223−4233.
(10) Vuceta, J.; Morgan, J. J. Chemical modeling of trace metals in fresh waters: Role of complexation and adsorption. *Environ. Sci. Technol.* **1978**, *12* (12), 1302−1309.
(11) Stone, A. T.; Morgan, J. J. Reduction and dissolution of Mn(III) and manganese(IV) oxides by organics. 2. Survey of the reactivity of organics. *Environ. Sci. Technol.* **1984**, *18* (8), 617−624.
(12) Scott, M. J.; Morgan, J. J. Reactions at oxide surfaces. 1. Oxidation of As(III) by synthetic birnessite. *Environ. Sci. Technol.* **1995**, *29* (8), 1898−1905.
(13) Wang, Y.; Stone, A. T. Reaction of $Mn^{III,IV}$ (hydr)oxides with oxalic acid, glyoxylic acid, phosphonoformic acid, and structurally-related organic compounds. *Geochim. Cosmochim. Acta* **2006**, *70*, 4477−4490.
(14) King, D. W. Role of carbonate speciation on the oxidation rate of Fe(II) in aqueous systems. *Environ. Sci. Technol.* **1998**, *32*, 2997−3003.
(15) Morgan, J. J. Chemical equilibria and kinetic properties of manganese in natural waters. In *Principles and Applications of Water Chemistry*; Faust, S. D., Hunter, J. V., Eds.; Wiley: New York, 1967; pp 561−624.
(16) Davies, S. H. R.; Morgan, J. J. Manganese (II) oxidation kinetics on metal oxide surfaces. *J. Colloid Interface Sci.* **1989**, *129* (1), 63−77.
(17) Von Langen, P. J.; Johnson, K. S.; Coale, K. H.; Elrod, V. A. Oxidation kinetics of manganese (II) in seawater at nanomolar concentrations. *Geochim. Cosmochim. Acta* **1997**, *61* (23), 4945−4954.
(18) Kessick, M. A.; Morgan, J. J. Mechanisms of autooxidation of manganese in aqueous solution. *Environ. Sci. Technol.* **1975**, *9* (2), 157−159.
(19) Hem, J. D. *Chemistry of Manganese in Natural Water: Chemical Equilibria and Rates of Manganese Oxidation*; U.S. Geological Survey Water Supply Paper, 1667-A; 1963; 64 pp.
(20) Matsui, I. *Catalysis and kinetics of manganous ion oxidation in aqueous solution and adsorbed on the surfaces of solid oxides*. Ph.D. thesis, Lehigh University, Bethlehem, PA, 1973.
(21) Sung, W. *Catalytic effects of the γ-FeOOH (lepidocrocite) surface on the oxygenation removal kinetics of Fe(II) and Mn(II)*. Ph.D. thesis, California Institute of Technology, Pasadena, CA, 1980.
(22) Pankow, J. F.; Morgan, J. J. Kinetics for the aquatic environment. *Environ. Sci. Technol.* **1981**, *15* (11), 1306−1313.
(23) Luther, G. W., III. *Inorganic Chemistry for Geochemistry and Environmental Sciences: Fundamentals and Applications*; Wiley: West Sussex, UK, 2016.
(24) Sung, W.; Morgan, J. J. Kinetics and products of ferrous iron oxygenation in aqueous systems. *Environ. Sci. Technol.* **1980**, *14*, 561−568.
(25) Mata-Perez, F.; Perez-Benito, J. F. The kinetic rate law for autocatalytic reactions. *J. Chem. Educ.* **1987**, *64* (11), 925−927.
(26) Wilson, D. E. Surface and complexation effects on the rate of Mn(II) oxidation in natural waters. *Geochim. Cosmochim. Acta* **1980**, *44*, 1311−1317.
(27) Morgan, J. J.; Smith, J. J. Chemical behavior of iron and manganese in natural waters. In *Proceedings of the Fourteenth Southern Water Resources and Pollution Control Conference*; Chapel Hill: NC, 1965; pp 148−164.
(28) Klewicki, J. K.; Morgan, J. J. Kinetic behavior of Mn(III) complexes of pyrophosphate, EDTA, and citrate. *Environ. Sci. Technol.* **1998**, *32* (19), 2916−2922.
(29) Duckworth, O. W.; Sposito, G. Siderophore-manganese(III) interactions. I. Air-oxidation of manganese(II) promoted by desferrioxamine B. *Environ. Sci. Technol.* **2005**, *39* (16), 6037−6044.
(30) Parker, D. L.; Morita, T.; Mozafarzadeh, M. L.; Verity, R.; McCarthy, J. K.; Tebo, B. M. Inter-relationships of MnO_2 precipitation, siderophore-$Mn^{(III)}$ complex formation, siderophore degradation, and iron limitation in $Mn^{(II)}$-oxidizing bacterial cultures. *Geochim. Cosmochim. Acta* **2007**, *71*, 5672−5683.
(31) Kostka, J. E.; Luther, G. W., III; Nealson, K. H. Chemical and biological reduction of Mn(III)-pyrophosphate complexes: Potential importance of dissolved Mn(III) as an environmental oxidant. *Geochim. Cosmochim. Acta* **1995**, *59* (5), 885−894.
(32) Oldham, V. E.; Mucci, A.; Tebo, B. M.; Luther, G. W., III Soluble Mn(III)-L complexes are abundant in oxygenated waters and stabilized by humic ligands. *Geochim. Cosmochim. Acta* **2017**, *199*, 238−246.
(33) Klewicki, J. K.; Morgan, J. J. Dissolution of β-MnOOH particles by ligands: Pyrophosphate, ethylenediaminetetraacetate, and citrate. *Geochim. Cosmochim. Acta* **1999**, *63* (19/20), 3017−3024.
(34) Peña, J.; Duckworth, O. W.; Bargar, J. R.; Sposito, G. Dissolution of hausmannite (Mn_3O_4) in the presence of the

trihydroxamate siderophore desferrioxamine B. *Geochim. Cosmochim. Acta* **2007**, *71*, 5661−5670.
(35) Stone, A. T. Microbial metabolites and the reductive dissolution of manganese oxides: Oxalate and pyruvate. *Geochim. Cosmochim. Acta* **1987**, *51*, 919−925.
(36) McArdell, C. S.; Stone, A. T.; Tian, J. Reaction of EDTA and related aminocarboxylate chelating agents with $Co^{III}OOH$ (Heterogenite) and $Mn^{III}OOH$ (Manganite). *Environ. Sci. Technol.* **1998**, *32* (19), 2923−2930.
(37) Kessick, M. A.; Vuceta, J.; Morgan, J. J. Spectrophotometric determination of oxidized manganese with leuco crystal violet. *Environ. Sci. Technol.* **1972**, *6* (7), 642−644.
(38) Johnson, D.; Chiswell, B. A new method for the evaluation of the oxidizing equivalent of manganese in surface freshwaters. *Talanta* **1993**, *40* (4), 533−540.
(39) Martell, A. E.; Smith, R. M. Critically Selected Stability Constants of Metal Complexes; *NIST Standard Reference Database 46*, Version 8, U.S. Department of Commerce: Gaithersburg, MD, 2004.
(40) Morel, F. M. M.; Hering, J. G. *Principles and Applications of Aquatic Chemistry*; Wiley-Interscience: New York, 1993.
(41) Gustafsson, J. P. *Visual MINTEQ*, ver. 3.1, Department of Land and Water Resources Engineering, Royal Institute of Technology-KTH, Stockholm, Sweden, available at https://vminteq.lwr.kth.se/.
(42) Bilinski, H. Precipitation and complex formation in the system $Mn(ClO_4)_2$-$Na_4P_2O_7$-pH (295 K, I = 0.5 and I $\asymp$ 0 mol dm^{-3}). *Polyhedron* **1983**, *2* (5), 353−358.
(43) Wang, Z.; Xiong, W.; Tebo, B. M.; Giammar, D. E. Oxidative UO_2 dissolution induced by soluble Mn(III). *Environ. Sci. Technol.* **2014**, *48*, 289−298.
(44) Hansard, S. P.; Easter, H. D.; Voelker, B. M. Rapid reaction of nanomolar Mn(II) with superoxide radical in seawater and simulated freshwater. *Environ. Sci. Technol.* **2011**, *45*, 2811−2817.
(45) Luther, G. W., III The role of one- and two-electron transfer reactions in forming thermodynamically unstable intermediates as barriers in multi-electron redox reactions. *Aquat. Geochem.* **2010**, *16* (3), 395−420.
(46) Cabelli, D. E.; Bielski, B. H. J. Pulse radiolysis study of the kinetics and mechanisms of the reactions between manganese(II) complexes and HO_2/O_2^- radicals. 1. Sulfate, formate, and pyrophosphate complexes. *J. Phys. Chem.* **1984**, *88* (14), 3111−3115.
(47) Learman, D. R.; Voelker, B. M.; Madden, A. S.; Hansel, C. M. Constraints on superoxide mediated formation of manganese oxides. *Front. Microbiol.* **2013**, *4*, 262.
(48) Andeer, P. F.; Learman, D. R.; McIlvin, M.; Dunn, J. A.; Hansel, C. M. Extracellular haem peroxidases mediate Mn(II) oxidation in a marine *Roseobacter* bacterium via superoxide production. *Environ. Microbiol.* **2015**, *17* (10), 3925−3936.
(49) Godwin, C. M.; Zehnpfennig, J. R.; Learman, D. R. Biotic and abiotic mechanisms of manganese (II) oxidation in Lake Erie. *Front. Environ. Sci.* **2020**, *8*, 57.
(50) Groschen, G. E.; Arnold, T. L.; Morrow, W. S.; Warner, K. L. Occurrence and distribution of iron, manganese, and selected trace elements in ground water in the glacial aquifer system of the Northern United States; *U.S. Geological Survey Scientific Investigations Report 2009−5006*; 2008; 89 pp.
(51) Smith, S. A. Beyond toxins: A source-to-treatment strategy for harmful algal blooms. *J. - Am. Water Works Assoc.* **2019**, *111*, 14−22.
(52) Crittenden, J. C.; Trussell, R. R.; Hand, D. W.; Howe, K. J.; Tchobanoglous, G. *MWH's Water Treatment Principles and Design*, 3rd Ed.; John Wiley & Sons, Inc.: Hoboken, NJ, 2012.

https://doi.org/10.1021/acs.est.1c01795
Environ. Sci. Technol. 2021, 55, 14426−14435